RSC Advances

PAPER

View Article Online
View Journal | View Issue

Cite this: *RSC Adv.*, 2021, **11**, 22390

Highly efficient and selective supramolecular hydrogel sensor based on rhodamine 6G derivatives

Zixiang Qu,[a] Chuane Wang,[a] Hongdong Duan *[a] and Liqun Chi*[b]

Received 28th December 2020
Accepted 7th June 2021

DOI: 10.1039/d0ra10890a

rsc.li/rsc-advances

A mercury ion sensitive fluorescent functional monomer was synthesized based on rhodamine 6G, and two highly-effective approaches about the research and development of novel macroscopic hydrogel sensor were reported. The monomer was utilized to synthesize hydrogel sensors by free radical polymerization and guest–host interaction. Hydrogel sensors have prominent selectivity to Hg^{2+} and can be tailored and reused, which are capable of detecting Hg^{2+} sensitively in flowing and standing water environment with satisfactory performance. This work is expected to open an avenue to construct novel fluorescent analysis method for Hg^{2+} detection.

1. Introduction

Due to its high sensitivity, excellent selectivity and convenient preparation, supramolecular hydrogel, an outstanding and promising smart polymer, has been exploited to escalate the functionality of traditional sensing materials.[1] In comparison with natural hydrogel, proteins and other supramolecular materials,[2] synthetic hydrogels function in a more convenient and better way during synthesis and can be used more widely among sensing materials.[3] Currently, responsive hydrogels functioning as the detector and recognizer of peculiar samples are of remarkable potentials for the research of micro actuators for micromanipulation in the microenvironment polluted by heavy metals.[4]

Mercury(II), one kind of the most toxic heavy metal ion, is contaminating extensively various natural environments and impacting human activities. It has raised extensive public concerns due to its adverse effect on environmental safety and human health.[5] More seriously, through the biological accumulation in human body, mercury ions may potentially affect the nervous system, causing malign illness. Accordingly, it is essential to develop a rapid, convenient and efficient Hg^{2+} detection method. Therefore, the design and fabrication of hydrogel systems with Hg^{2+} responsive characteristic as the micro actuator for micromanipulation in Hg^{2+} polluted microenvironment are highly required, which are of profound and significant value in scientific research and technological development.[6]

Currently, a multielement composite materials synthesized under the basis of macroscopic macromolecular hydrogels were conducted into full investigation with the purpose of optically detecting and monitoring diverse metal ions.[7] By hydrogel sensors, the detection of metal ions in natural environment is regarded as an easily manipulated and low-cost analytical method with simple process and prominent sensitivity. Without spectroscopic equipment, it is still feasible to directly analyze target ions by naked eyes through researches.[8–11] Therefore multifarious synthetic strategies of hydrogel sensors have been researched, designed and developed throughout their functionalization procedures, performance control and potential applications. Peculiarly, the sensor systems through colorimetric and fluorometric detection by naked eyes without equipment necessity will be of great and extensive utility, for these hydrogel sensors are easy to operate and contain eminent sensitivity and high signal–noise-response ratio.[12–16] Furthermore, these low-costed materials can be easily prepared and are of prominent convenience to be adapted in diverse conditions.

In order to overcome the shortcomings of traditional fluorescence detection method such as monitoring limitation, detection condition and human errors, hydrogel immobilized sensors with response signals which are available for current living environment make the detection operation more convenient and produce more convincing and urgently needed detection results.[17] Therefore, developing hydrogel sensor to detect Hg^{2+} with colorimetric and fluorescence dual signals is of great importance. The successful synthesis of hydrogel sensors will derive widespread opportunities for practical applications in luminescent patterning, manufacturing of subaqueous fluorescent devices, sensors and bioengineering.[18] In consideration of the law of nature, applying soft materials on the research and development of manual artificial coloring will boost the diversity and universality of practical utility.[19–21]

In this study, rhodamine 6G-based derivative was selected as the fluorophore by structural modifications and the thiophene was selected as the recognition site of Hg^{2+}. Accordingly, the

[a]*School of Chemistry and Chemical Engineering, Qilu University of Technology (Shandong Academy of Sciences), Jinan, Shandong Province, 250353, China. E-mail: hdduan67@163.com; Tel: +86 13153035598*

[b]*Department of Pharmacy, Haidian Maternal & Child Health Hospital of Beijing, Haidian, Beijing, 100080, China*

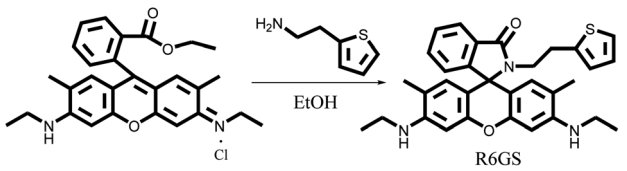

Scheme 1 Synthesis of R6GS.

novel fluorescence probe **R6GS** was designed and synthesized and **R6GS** performed ideal properties in Hg^{2+} detection. Two types of optical hydrogel sensors with fluorescence responsiveness in sensing Hg^{2+} were synthesized by exploiting this probe. When hydrogel sensors were exposed to Hg^{2+} aqueous solution, the hydrogels shifted from achromatic color to red and the intensity as well as Hg^{2+} concentration remained positively correlated. In principle, the hydrogel sensor featured selective and integral detection and monitoring of Hg^{2+}. The effective approach developed two novel macroscopic hydrogel sensors, which formed an easily manipulated, intelligent and aqueous environment adaptive sensing devices.

2. Experiment method

2.1. Material and instrumentation

Rhodamine 6G was purchased from Aladdin Co. Ltd. All chemical reagents satisfied the requirements of analytical grade or reached the highest purity availability, which were utilized without the necessity of further purification. The preparation of metal ions solutions was in deionized water. By using DMSO-d_6 as the solvent and tetramethylsilane (TMS) as the internal reference, Bruker-AVANCE 400 NMR Spectrometer was utilized to record ^{1}H and ^{13}C NMR spectra. FT-IR spectra were observed on Thermo fisher Nicolet 6700 FT-IR spectrophotometer. High Resolution Mass Spectra (HRMS) were measured on Accurate-Mass Q-TOF LC/MS system. Shimadzu UV-2600 spectrophotometer was used to record UV-Vis absorption spectra. Fluorescence spectra were gauged on Hitachi F-4600 which functions as the measurement of fluorescent intensity.

2.2 Synthesis process of R6GS

Rhodamine 6G (0.4790 g, 1.0 mmol) and 2-thiopheneethylamine (0.1399 g, 1.1 mmol) were dissolved in 70 mL EtOH, among which the mixture was stirred under reflux for 6 hours. The solvent was concentrated by reducing pressure and the mixture was purified through chromatography (dichloromethane/ethanol = 40/1, v/v) successively. The goal product, **R6GS**, was obtained as the light pink solid (0.3608 g, yield = 77%). The synthesis of **R6GS** showed in Scheme 1. ^{1}H NMR (400 MHz, DMSO-d_6, ppm): δ 7.84–7.74 (m, 1H), 7.53 (p, J = 7.7 Hz, 2H), 7.23 (t, J = 9.6 Hz, 1H), 7.09–6.98 (m, 1H), 6.88–6.78 (m, 1H), 6.62 (d, J = 3.0 Hz, 1H), 6.29 (s, 2H), 6.07 (s, 2H), 5.09 (t, J = 5.3 Hz, 2H), 3.24–3.03 (m, 6H), 2.47 (s, 2H), 1.88 (d, J = 18.9 Hz, 6H), 1.21 (t, J = 7.1 Hz, 6H). ^{13}C NMR (101 MHz, DMSO-d_6, ppm) δ 166.90, 151.50, 148.46, 145.70, 144.73, 142.87, 141.08, 138.03, 136.79, 131.70, 128.24, 124.70, 118.90, 114.00, 105.01, 89.67, 79.79, 65.01, 37.93, 32.40, 17.62, 14.57. FT-IR: (KBr, cm^{-1}) ν 3477(N–H) 1624 (C=O) 1294 (C=C), HRMS (ESI): $C_{32}H_{33}N_3O_6S$ calculated for: 523.2293; found 524.2339 for $[M+H]^+$.

2.3 General processes of spectroscopic analysis of R6GS

The standard stock solution of metal ions (Na^+, K^+, Ca^{2+}, Fe^{2+}, Fe^{3+}, Co^{2+}, Ni^{2+}, Cu^{2+}, Zn^{2+}, Pb^{2+}, Cd^{2+}, Mn^{2+}, Ba^{2+}, Mg^{2+} and Hg^{2+}) was diluted with deionized water to generate 10^{-3} M solutions for optical properties experiments. 1 M of ethylenediamine (EDA) solvent was added in purified water. The preparation of stock solution (10^{-3} M) was conducted by dissolving **R6GS** in DMSO, and the mixed solution of DMSO/H_2O was used to dilute **R6GS** solution in order to obtain the analytical solution (DMSO/H_2O = 9/1, v/v). The pH scope of solutions was allocated and adjusted by 4 M hydrochloric acid aqueous solution or 4 M sodium hydroxide aqueous solution.

2.4 Synthesis of hydrogel sensors

Hydrogel sensors were synthesized by means of free radical polymerization (Fig. 1). In DMSO solution, AAm, MMA, **R6GS** and MBA (0.3% of monomer content) were firstly dissolved and mingled with each other. Under high vacuum environment, the mixture was stirred continuously at 15 °C until the homogeneous solution was formed. In the subsequent step, the mixture was added by 100 μL TEMED and initiator (APS, 2% monomer) which were mixed and dissolved in 2.0 mL of DMSO. The mixture was stirred constantly until the homogeneous solution was witnessed in the reaction, at which time the solution was poured into a cylindrical mould and maintained at 50 °C for 12

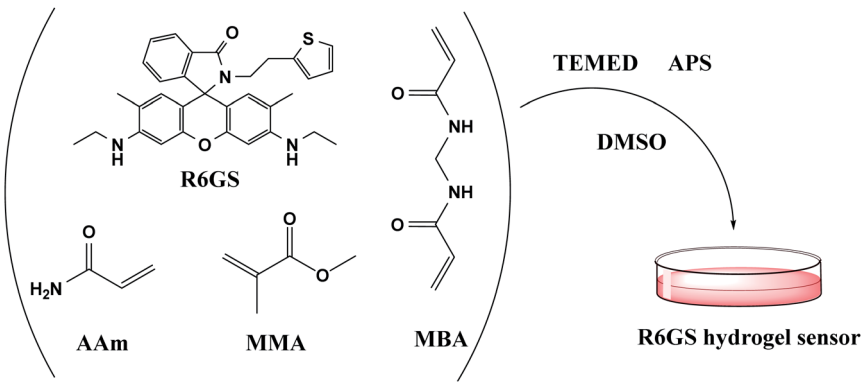

Fig. 1 Synthesis of hydrogel sensor by free radical polymerization.

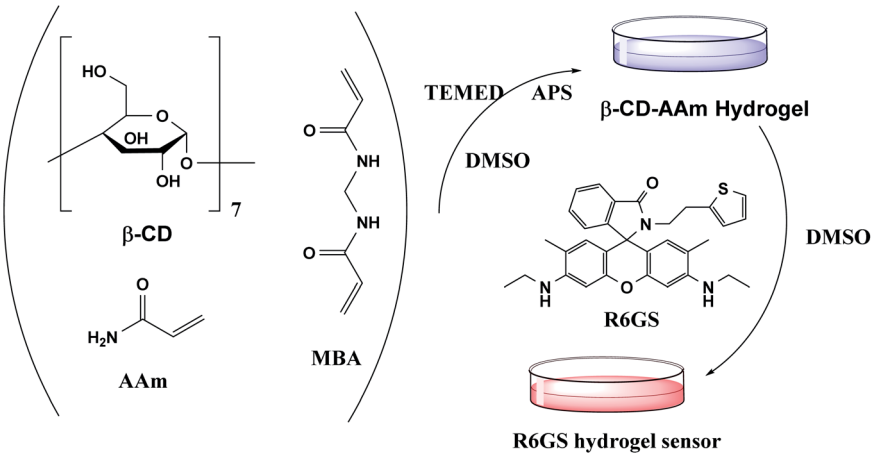

Fig. 2 Synthesis of hydrogel sensor by guest–host interaction.

hours accordingly. Hydrogel sensors were hereby extracted from the mould and washed by DMSO for 36 hours and then by distilled water for 36 hours. At this moment, one piece of the hydrogel was separated and dried in an oven at 50 °C for the research of swelling kinetics of hydrogel sensors.

In addition, synthesized supramolecular hydrogels can be used to fabricate hydrogel sensors by guest–host interaction (Fig. 2). At first, AAm, β-CD and MBA (0.3% of monomer content) were commonly stirred in dimethylsulfoxide. The mixed solvent was fully dispersed under vacuum at 5 °C. In the following step, the mixture was added by 100 μL of TEMED and initiator (APS, 4% of monomer content). The mixture was stirred constantly until the homogeneous solution was witnessed in the reaction, at which time the solution was poured into a cylindrical mould and was maintained at 50 °C for 12 hours accordingly. The hydrogel was thereby extracted from the mould and washed by DMSO for 36 hours. Then, on the basis of the host–guest interaction, AAm-*co*-β-CD hydrogel was immersed in 10^{-2} M **R6GS** DMSO solution for 10 hours to assemble hydrogel sensor.

3. Results and discussion

3.1. Optical properties of R6GS

The investigation of UV-Vis spectra of **R6GS** with regard to various metal ions (Na^+, K^+, Ca^{2+}, Fe^{2+}, Fe^{3+}, Co^{2+}, Ni^{2+}, Cu^{2+}, Zn^{2+}, Pb^{2+}, Cd^{2+}, Mn^{2+}, Ba^{2+}, Mg^{2+} and Hg^{2+}) was initiated on UV-Vis spectroscopy, as shown in Fig. 3. Notably the absorption band of **R6GS** (10^{-4} M, DMSO/H_2O, 9/1, v/v) solution reached at 275–700 nm after investigation, and a clear absorption band that reached at 308 and 538 nm appeared after adding Hg^{2+}. The result demonstrated that **R6GS** responded selectively to Hg^{2+}. However, no other obvious absorption band was shown after adding other metal ions, which proved the superior selectivity of **R6GS** toward Hg^{2+}.

The investigation of fluorescence emission behavior of **R6GS** toward different metal ions (K^+, Na^+, Ca^{2+}, Fe^{2+}, Fe^{3+}, Ba^{2+}, Mn^{2+}, Co^{2+}, Zn^{2+}, Cu^{2+}, Ni^{2+}, Cd^{2+}, Pb^{2+}, Mg^{2+} and Hg^{2+}) was initiated in DMSO/H_2O (9/1, v/v) solutions, as shown in Fig. 4.

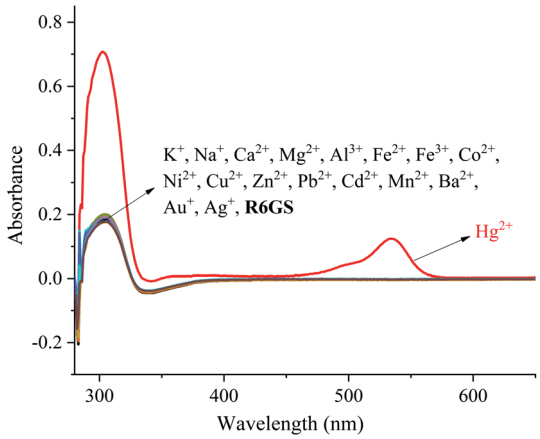

Fig. 3 UV-Vis spectral of **R6GS** (10^{-4} M) in DMSO/H_2O (9/1, v/v).

No obvious fluorescence emission was shown from the standard solution of **R6GS** in DMSO/H_2O (9/1, v/v), however the addition of Hg^{2+} enhanced a significant fluorescence display with the emission maximum at 581 nm. Accordingly, the blocked

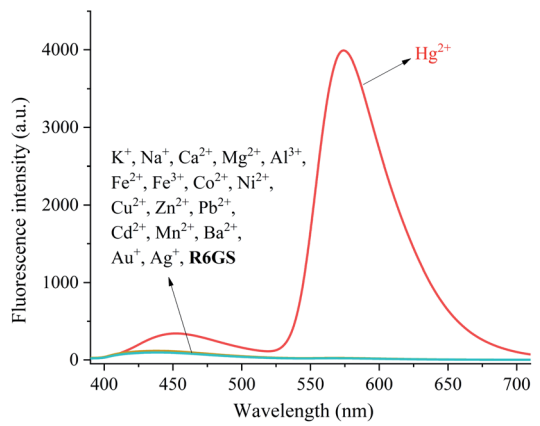

Fig. 4 Fluorescence spectra of **R6GS** in the presence of different testing species (10^{-5} M) in DMSO/H_2O (9/1, v/v) (λ_{ex} = 360 nm).

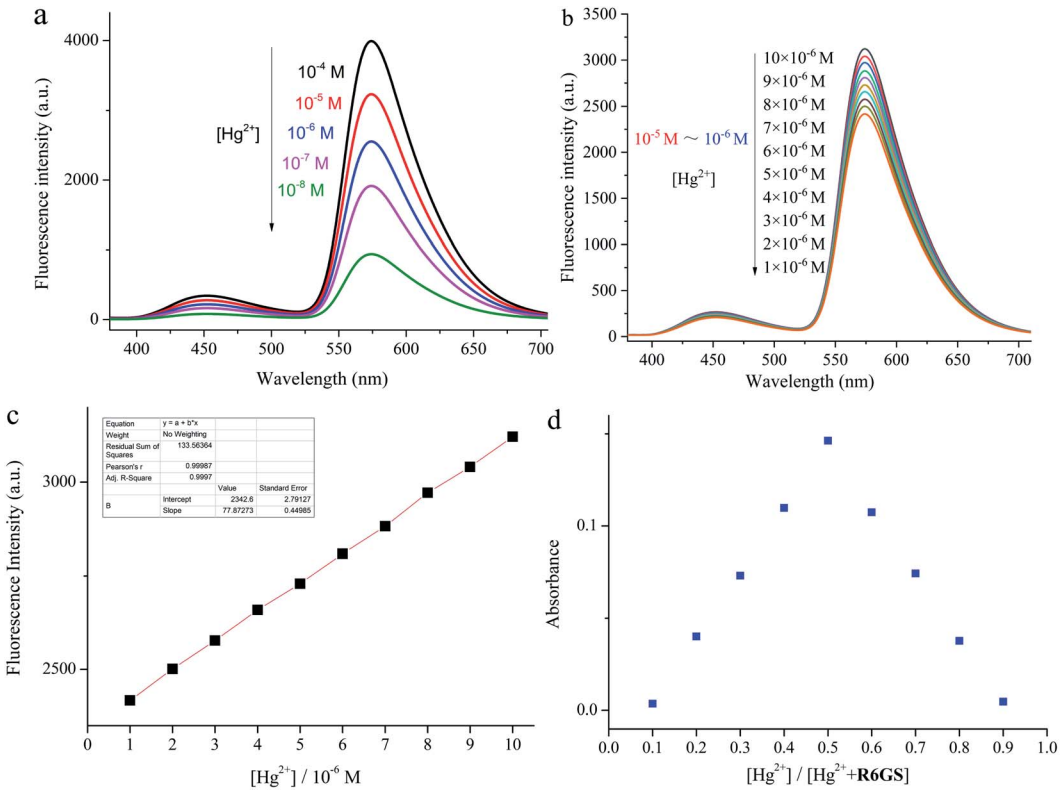

Fig. 5 (a) Fluorescence spectra of **R6GS** with different concentration of Hg^{2+} (DMSO/H_2O = 9/1, v/v, λ_{ex} = 360 nm), (b) fluorescence spectra of **R6GS** with 10^{-5} M to 10^{-6} M of Hg^{2+} (DMSO/H_2O = 9/1, v/v, λ_{ex} = 360 nm), (c) calculation of detection limits of **R6GS** for Hg^{2+} (DMSO/H_2O = 9/1, v/v), (d) Job's plot of **R6GS**.

photoinduced electron transfer (PET) and the chelation-enhanced fluorescence (CHEF) process acted as the inducement of these consequences. With regard to experimental comparison, no obvious change was shown on the fluorescence spectra after adding other metal ions. Thus the result demonstrated prominent fluorescent selectivity of **R6GS** toward Hg^{2+}.

3.2. Sensitivity and selectivity of R6GS

The rapid detection and response of **R6GS** to Hg^{2+} as well as the notable intensity of the fluorescence display could be attributed to the blocked PET process and CHEF. On account of quenching by rhodamine 6G hydrazide derivatives through PET, **R6GS** displayed a very weak fluorescence band at 581 nm. Meanwhile the bonding process between Hg^{2+} and probe **R6GS** and the complex opening procedure of spirolactam ring were witnessed, accompanying with the blocking of the PET process. The rigidity of sensor molecules triggered CHEF effect by stable complexation while suppressing the PET process, which resulted in the intensification of fluorescence display. The Job's plot was shown in Fig. 5d. The generation of 1 : 1 complex between **R6GS** and Hg^{2+} was demonstrated from the result and the Detection Limit (DL) was therefore confirmed (Fig. 5b). As shown in Fig. 5c, the DL of Hg^{2+} was 25.7 nm. The results thereby demonstrated that **R6GS** was highly sensitive to Hg^{2+} and was available to synthesize fluorescent sensing materials (Fig. 5a).

3.3. Detection mechanism of R6GS

Based upon Job's plots and the investigation of FT-IR spectra, the proposed binding mechanism was shown in Scheme 2. On account of the PET process, the fluorescence display in free solution of **R6GS** was weak. However, when Hg^{2+} was added, the

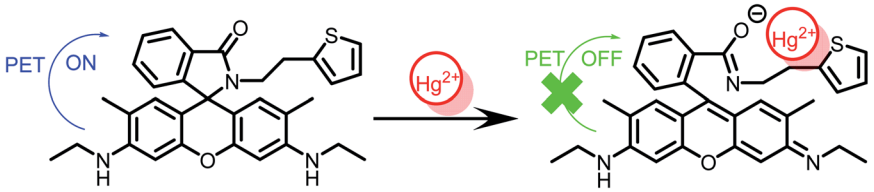

Scheme 2 Sensing process of **R6GS** to Hg^{2+}.

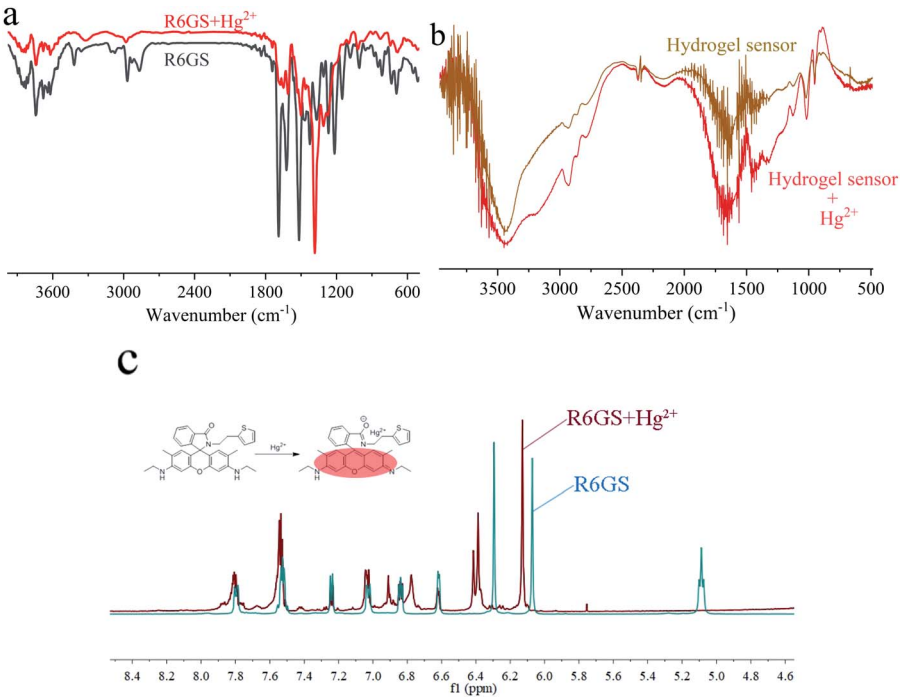

Fig. 6 (a) FT-IR spectrum of **R6GS** and **R6GS**–Hg^{2+} (b) FT-IR spectrum of hydrogel sensor and hydrogel sensor–Hg^{2+} (c) ^1H NMR spectra of **R6GS** and **R6GS**–Hg^{2+}.

PET process was hindered owing to the ring opening of lactam, which strongly intensified fluorescence display and triggered noticeable color variation. The proposed hydrogel sensor binding mechanism was similar to **R6GS**'s.

Through FT-IR spectra, the binding modes of **R6GS**–Hg^{2+} were established and studied. The FT-IR spectra of **R6GS** and **R6GS**–Hg^{2+} were shown in Fig. 6a. Fig. 6b showed the FT-IR spectra of hydrogel sensor and hydrogel sensor–Hg^{2+}. Through research and observation, the characteristic of N–H bands of the compound reached at 3419 and 2926 cm^{-1} and the C=O stretching frequencies of the compound reached at 1647 cm^{-1} for lactam. After **R6GS** chelated with Hg^{2+}, the peak of the aromatic C=C stretching band significantly changed and the C=O peak shifted to 1537 cm^{-1}. Through research and observation, C=N peak obviously shifted to 1383 cm^{-1}, which promoted the ring opening process of the N-(rhodamine 6G) lactam in **R6GS**. Meanwhile ^1H NMR spectra of **R6GS** and **R6GS**–Hg^{2+} were observed and shown in Fig. 6c (400 MHz, DMSO-d_6). Within δ 6.0–8.0 ppm, **R6GS** performed 8 sorts of signals. After Hg^{2+} was added to **R6GS**, the aromatic and methyl protons of xanthene underwent pronounced downfield chemical shifts, which proved the delocalization of xanthene and supported that the large fluorescence enhancement could be attributed to the spirolactam ring opening.

3.4. The research of R6GS reversibility

Through investigation, adding EDA solution (Fig. 7a) promoted the reversibility of the **R6GS** detection process. In **R6GS** and Hg^{2+} mixture, the diminution of fluorescence intensity and the

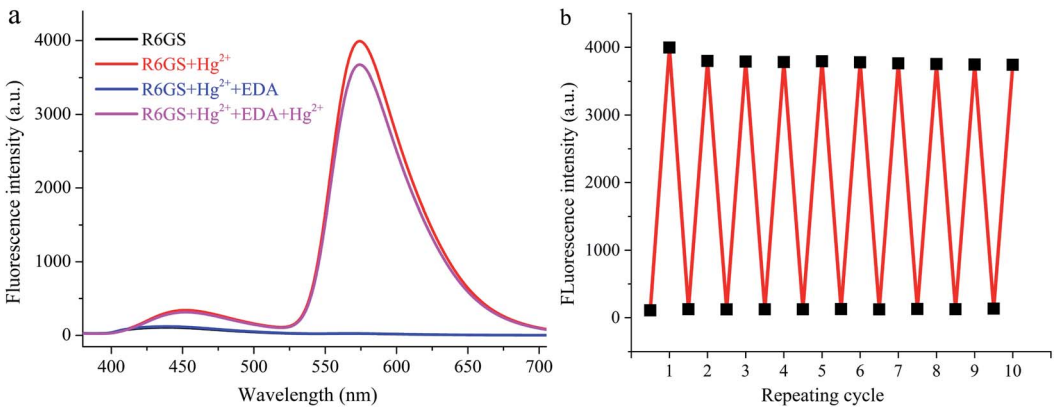

Fig. 7 (a) Fluorescence reversibility of **R6GS** (λ_{ex} = 360 nm, DMSO/H_2O = 9/1, v/v) (b) repeatability of Hg^{2+} sensing behavior of **R6GS** (λ_{ex} = 360 nm, DMSO/H_2O = 9/1, v/v).

recovery of fluorescence indication of **R6GS** could be ascribed to the addition of EDA solution. Meanwhile, the change of solution color from fluorescent red to transparent demonstrated the regeneration of the free sensor **R6GS**, and Hg^{2+} could still be responded by the regenerated sensor. Fig. 7b indicated that **R6GS** can be used as the reversible colorimetric sensor for Hg^{2+} in aqueous solution. Characteristics such as the reversibility and the regeneration of the sensor are of profound and vital significance for the development of effective sensor for Hg^{2+} in aqueous environment.

3.5. The pH effect

The influence of the probe **R6GS** to Hg^{2+} in different pH environments was investigated. As shown in Fig. 8, in the range of pH 3.0–4.0, the probe could not respond visibly to Hg^{2+}. In the range of pH 5.0–8.0, the Hg^{2+} could respond effectively to Hg^{2+} without dramatic pH influence. The fluorescence intensity of the response of the probe to Hg^{2+} at 581 nm was gradually weakened as the pH value improved to the range of 8.0–9.0. This phenomenon could be attributed to the fluorescence enhancement that was caused by the disruption of the spirolactam of **R6GS** in acidic environment (pH < 4), while the bonding process between Hg^{2+} and **R6GS** was inhibited, no sensing reaction was caused in alkaline environment (pH ≥ 9). And thus the results indicated that the probe **R6GS** displayed well fluorescent response to Hg^{2+} in weak acidic to weak alkaline environment.

3.6. The fabrication of hydrogel sensor

In this work, ^{1}H NMR conspicuously demonstrated the formation of β-CD-**R6GS** inclusion complex, and the work preliminarily elucidated and clearly illustrated the inclusion process. During the absence and presence of **R6GS**, Fig. 9 presented the ^{1}H NMR spectra of β-CD. The integral intensities of the signals in the ^{1}H NMR spectra were analyzed. The inclusion of **R6GS** exhibited slight changes in β-CD as well as profoundly influenced the chemical shift of β-CD protons. Furthermore, the chemical shift of β-CD protons fluctuated obviously (Table 1),

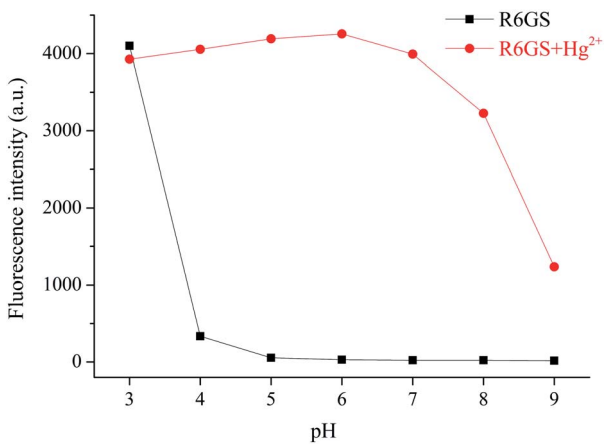

Fig. 8 Fluorescence response of R6GS as the function of pH (3.0–9.0) during the absence and presence of Hg^{2+} (DMSO/H_2O = 9/1, v/v, λ_{ex} = 360 nm).

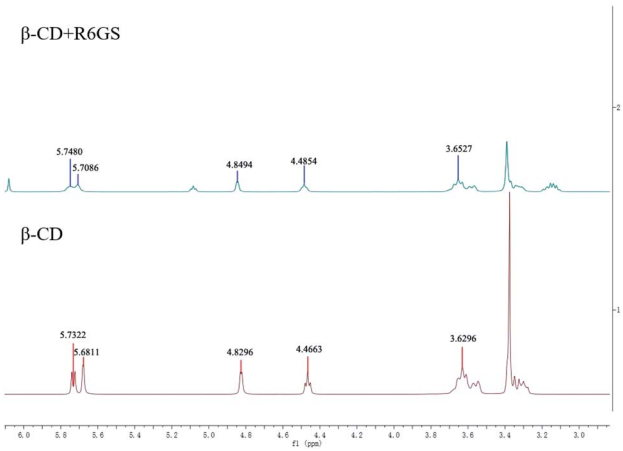

Fig. 9 ^{1}H NMR spectra of pure β-CD and β-CD + R6GS.

which illustrated that these protons mainly effected the inclusion of **R6GS**. ^{1}H NMR studies produced more supporting evidences for the inclusion of **R6GS** into the central cavity of β-CD. In comparison of free β-CD and **R6GS**, the mutual interaction between **R6GS** and β-CD was illustrated by the appearance of the chemical shifts of the inclusion complex.

3.7. Detection performance of hydrogel sensors

Optical properties experiments were carried out (Fig. 10) to study the selectivity of the conjugation of β-CD + **R6GS**. In consideration of experimental comparison, the complex of β-CD–**R6GS** did not affect the recognition and sensing performance of the probe molecules, thus the result demonstrated that after bonding with β-CD, **R6GS** still performed superior selectivity toward Hg^{2+}.

On the basis of PET and CHEF, hydrogel sensors obtained by two preparation methods demonstrated their prominent responsiveness, selectivity and sensitivity for Hg^{2+}. Aiming at the confirmation of the capability of hydrogel sensor, the determination of hydrogels detection limits (DL) was finished in different concentrations (from 10^{-3} M to 10^{-8} M) of Hg^{2+} solutions. When the concentration of Hg^{2+} reached 10^{-7} M, the color of hydrogel sensor could still be observed notably. With regard to the response time of detection and confirmation, color change of the hydrogel began in 20 min with 3 mm of thickness, among which the concentration of Hg^{2+} was 10^{-6} M. Meanwhile the hydrogel color changed when the concentration of Hg^{2+} was 10^{-3} M, 10^{-4} M and 10^{-5} M in 40 s, 2 min and 10 min respectively, as shown in Fig. 11 and 12. In aqueous solution environment, the hydrogel sensor showed visible red light (same

Table 1 ^{1}H NMR chemical shifts (δ, ppm) of pure β-CD and β-CD + R6GS

Proton	1	2	3	4	5
β-CD	5.7322	5.6811	4.8296	4.4663	3.6296
β-CD + **R6GS**	5.7480	5.7086	4.8494	4.84	3.6527

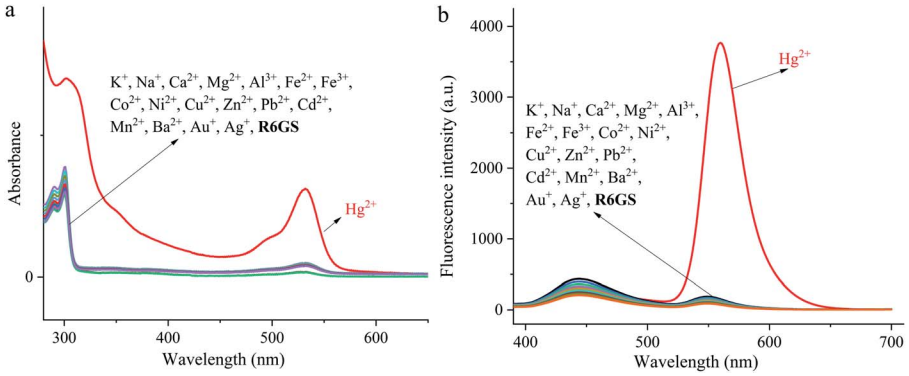

Fig. 10 (a) UV-Vis spectral of β-CD + **R6GS** in the presence of different testing species (β-CD : **R6GS** = 1 : 1, 10^{-4} M) in DMSO/H_2O (9/1, v/v) (b) fluorescence spectra of β-CD + **R6GS** in the presence of different testing species (β-CD : **R6GS** = 1 : 1, 10^{-5} M) in DMSO/H_2O (9/1, v/v) (λ_{ex} = 360 nm).

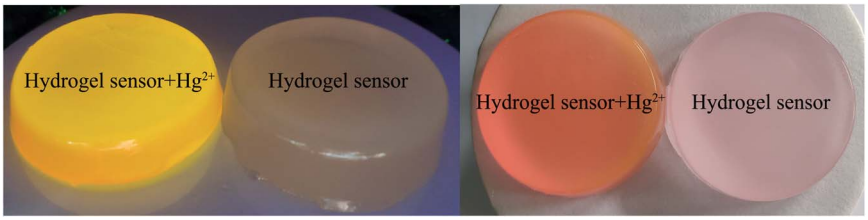

Fig. 11 The color changes of hydrogel sensor (synthesis by guest–host interaction) in the sensing process of Hg^{2+} under visible light and UV light at 365 nm.

with **R6GS**). Under 365 nm UV light, the color of hydrogel sensor changed more intensively in aqueous solution. Therefore, hydrogel sensors can be utilized as an easily manipulated platform with prominent detection performance to Hg^{2+}.

3.8. Universality of hydrogel sensors

According to the performance of hydrogel sensors in Hg^{2+} solution, the respective Hg^{2+} responses of hydrogel sensors in flowing water environment and standing water environment were further investigated. The hydrogel sensor colored from transparent to light aubergine (about 6 min) after being exposed to the flowing Hg^{2+} solution (10^{-4} M, 80–120 mL min^{-1}). The color changed to sharp aubergine after 10 min of exposure. In a 50 L glass jar, the hydrogel sensor was immersed in the standing Hg^{2+} solution, which resulted in an inspiring fact that when the gel was steeped in 10^{-8} M Hg^{2+} solution for 3 h, the color of the hydrogel sensor changed. This was beyond our expectation because in the detection performance experiment, hydrogel sensor showed no response to the small amount of Hg^{2+} solution whose concentration is under 10^{-8} M. From the experimental phenomenon, the summary is that the cumulative effect in hydrogel sensor may be generated, which can reduce the detection limit of probe to some extent. Thus this sensing performance of the hydrogel sensor may provide an approach for developing a kind of substantial, sustainable and fast-responsive test strip for the accurate detection of Hg^{2+} through naked-eye observation, which is particularly important in real-time Hg^{2+} monitoring in natural water environment and the liquid environment of chemical plants zone. Meanwhile, the naked-eye observation of color changes makes the detection of Hg^{2+} much faster and more convenient. Hence the technological proposal is a reliable alternative for the detection of Hg^{2+} in water environment.

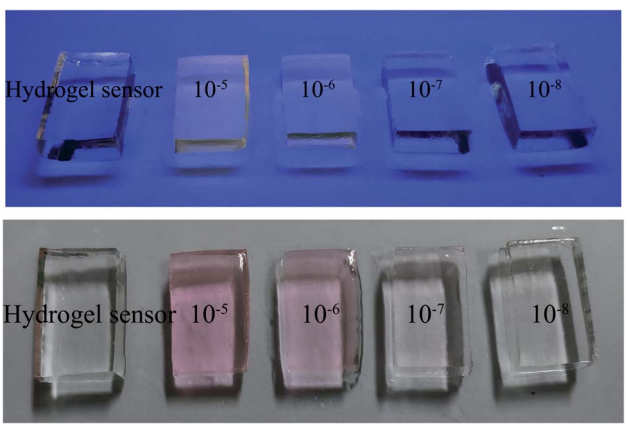

Fig. 12 The color changes of hydrogel sensor (synthesis by free radical polymerization) in the presence of different concentration of Hg^{2+} under visible light and UV light at 365 nm.

4. Conclusion

In summary, two easily manipulated and widely applicable synthesis strategies of Hg^{2+} responsive hydrogel sensor that is

characterized by fluorescent off–on switch and color convertibility were demonstrated. In water samples, hydrogel sensors have been successfully applied for tracking and determining the amounts of Hg^{2+}, which demonstrated that hydrogel sensors are suitable for common people and scientists under practical requirement. In addition, the method can be applied in a wide range of environments to build monitoring detection module and system, including flowing water environment detection system, standing water environment detection system, and so on. The method is expected to be capable of providing novel sights to explore smarter strategies that couple with synergistic functions of visual detection and efficient sensing.

Conflicts of interest

There are no conflicts to declare.

Acknowledgements

This work was funded by the Natural Science Foundation of Shandong Province (No. ZR2018PB007), the Shandong Provincial Natural Science Foundation of China (ZR2017LC005).

References

1 Z. Qu, L. Wang, S. Fang, D. Qin, J. Zhou, G. Yang and H. Duan, *Microchem. J.*, 2019, **150**, 104198.
2 T. Santaniello, L. Migliorini, Y. Yan, C. Lenardi and P. Milani, *J. Nanopart. Res.*, 2018, **20**, 250.
3 D. Görl, B. Soberats, S. Herbst, V. Stepanenko and F. Würthner, *Chem. Sci.*, 2016, **7**, 6786–6790.
4 S. Kampaengsri, B. Wanno, T. Tuntulani, B. Pulpoka and C. Kaewtong, *Environ. Technol.*, 2019, 1–7.
5 Y.-M. Liu, W. Wang, W.-C. Zheng, X.-J. Ju, R. Xie, D. Zerrouki, N.-N. Deng and L.-Y. Chu, *ACS Appl. Mater. Interfaces*, 2013, **5**, 7219–7226.
6 R. Wang, T.-S. Lin, J. A. Johnson and B. D. Olsen, *ACS Macro Lett.*, 2017, **6**, 1414–1419.
7 K. M. Lee, Y. Oh, J. Y. Chang and H. Kim, *J. Mater. Chem. B*, 2018, **6**, 1244–1250.
8 M. Qin, M. Sun, R. Bai, Y. Mao, X. Qian, D. Sikka, Y. Zhao, H. J. Qi, Z. Suo and X. He, *Adv. Mater.*, 2018, **30**, 1800468.
9 N. Kumari, N. Dey, S. Jha and S. Bhattacharya, *ACS Appl. Mater. Interfaces*, 2013, **5**, 2438–2445.
10 N. Kumari, N. Dey and S. Bhattacharya, *Analyst*, 2014, **139**, 2370–2378.
11 N. Kumari, N. Dey and S. Bhattacharya, *RSC Adv.*, 2014, **4**, 4230–4238.
12 J. Qin, B. Dong, X. Li, J. Han, R. Gao, G. Su, L. Cao and W. Wang, *J. Mater. Chem. C*, 2017, **5**, 8482–8488.
13 N. Dey, J. Kulhanek, F. Bures and S. Bhattacharya, *J. Org. Chem.*, 2019, **84**, 1787–1796.
14 N. Dey, D. Biswakarma, A. Ganguly and S. Bhattacharya, *ACS Sustainable Chem. Eng.*, 2018, **6**, 12807–12816.
15 S. K. Samanta and S. Bhattacharya, *J. Mater. Chem.*, 2012, **22**, 25277–25287.
16 S. Bhattacharya and M. Thomas, *Tetrahedron Lett.*, 2000, **41**, 10313–10317.
17 B. Dai, M. Cao, G. Fang, B. Liu, X. Dong, M. Pan and S. Wang, *J. Hazard. Mater.*, 2012, **219**, 103–110.
18 M. Moirangthem, R. Arts, M. Merkx and A. P. Schenning, *Adv. Funct. Mater.*, 2016, **26**, 1154–1160.
19 J. Zheng, P. Xiao, X. Le, W. Lu, P. Théato, C. Ma, B. Du, J. Zhang, Y. Huang and T. Chen, *J. Mater. Chem. C*, 2018, **6**, 1320–1327.
20 S. Bhattacharjee and S. Bhattacharya, *Chem. Commun.*, 2014, **50**, 11690–11693.
21 S. K. Samanta and S. Bhattacharya, *Chem. Commun.*, 2013, **49**, 1425–1427.